

See discussions, stats, and author profiles for this publication at: <https://www.researchgate.net/publication/40219439>

Catalytic Role of Calix[4]hydroquinone in Acetone–Water Proton Exchange: A Quantum Chemical Study of Proton Transfer via Keto–Enol Tautomerism

ARTICLE *in* THE JOURNAL OF PHYSICAL CHEMISTRY A · JANUARY 2008

Impact Factor: 2.69 · Source: OAI

CITATION

1

READS

13

3 AUTHORS, INCLUDING:



Artem E. Masunov

University of Central Florida

147 PUBLICATIONS 2,534 CITATIONS

SEE PROFILE



Andreas Dreuw

Universität Heidelberg

153 PUBLICATIONS 6,738 CITATIONS

SEE PROFILE

Catalytic Role of Calix[4]hydroquinone in Acetone–Water Proton Exchange: A Quantum Chemical Study of Proton Transfer via Keto–Enol Tautomerism

M. Zakharov,^{*,†,‡} A. E. Masunov,[§] and A. Dreuw^{*,†}

Institute of Physical and Theoretical Chemistry, Goethe University, Max von Laue Str 7, 60438 Frankfurt/Main, Germany, NMR Division, Max Planck Institute for Polymer Research, Postfach 3148, D-55021 Mainz, Germany, and Nanoscience Technology Center, Department of Chemistry, and Department of Physics, University of Central Florida, 12424 Research Parkway, Ste 400, Orlando, Florida 32826

Received: June 05, 2008; Revised Manuscript Received: July 24, 2008

Calix[4]hydroquinone has recently attracted considerable interest since it forms stable tubular aggregates mediated solely by hydrogen bonding and π – π -stacking interactions. These aggregates trap specifically various small organic molecules and, in particular, catalyze the proton exchange of water with acetone. Using correlated quantum chemical methods, the mechanism of the observed proton exchange mediated by keto–enol tautomerism of acetone is investigated in detail. Starting with an investigation of keto–enol tautomerism of acetone–water clusters, it appears that four catalytic water molecules are optimal for the catalysis and that additional solvent water molecules lead to a decrease in efficiency. Analyses of the partial charges revealed a decrease of the polarization of the reactive hydrogen bonds due to the additional water molecules. As a next step, hydroquinone–acetone–water complexes were studied as models for the situation in the CHQ moieties. However, the computations revealed that the proton transfer reaction becomes less efficient when one catalytic water molecule is replaced by hydroquinone. Although concerted proton transfer via keto–enol tautomerism of acetone seems to be the predominant mechanism in supercritical water, it is no longer the rate-determining reaction mechanism for the catalyzed acetone–water proton exchange observed in tubular CHQ. Nevertheless, a key feature of the catalytic function of tubular CHQ has been identified to be the stiff hydrogen bonding network and the exclusion of additional solvent water molecules.

1. Introduction

Over the past few decades, self-assembling organic hollow and tubular structures have attracted significant interest as prospective functional materials in the areas of catalysis, electrochemistry, molecular recognition, and drug discovery.¹ Most of the research in this field has been designated to the investigation of organic and inorganic nanotubes with covalently bound architectures. Recently, Kim and co-workers discovered and investigated the self-assembly phenomenon of calix[4]-hydroquinone (CHQ) monomers, which builds tubular nanostructures in the presence of water under certain experimental conditions (Figure 1).² These tubular structures are built from bowl-shaped nontubular CHQ monomers, which are not covalently bound but linked by hydrogen bonds (H-bond) with bridging water molecules. The bridging water molecules and –OH groups of the CHQ building blocks constitute a quasi one-dimensional (1D) H-bond chain along the axis of the tubular structure. The CHQ tubes aggregate further into bigger porous polymers mediated by intertubular π – π stacking interactions that laterally stabilize the tubular subunits. In contrast to covalently bound nanotubes, the ordering in organic CHQ nanotubes is stipulated by a delicate interplay of H-bonding and π – π interactions similar to the situation found in biological materials, like membranes and membrane proteins.³

The hollow bowl shape of the aromatic CHQ molecules allows for an efficient size-specific trapping of organic guest molecules and for their subsequent chemical transformation by, for example, stereoselective reactions.⁴ Moreover, a recent NMR/quantum chemical study has shown that CHQ nanotubes can specifically trap small organic molecules (acetone, 2-propanol, and 2-methyl-2propanol). In particular, it was demonstrated that in the case of acetone, one molecule fits into one CHQ bowl.^{4,5} Understanding the mechanism of the size-specific binding and the mobility of the guest molecules in CHQ nanotubes will give insights relevant also for trans-membrane ion channels and pore structures, due to their above-mentioned structural relation.³

An important manifestation of the unusual chemical properties of tubular CHQ structures is its catalytic function in acetone–water proton exchange (PE),⁶ which has been observed at ambient conditions in two NMR experiments, whose spectra are shown in Figure 2. In a solid state magic-angle spinning ¹H NMR experiment on the CHQ nanotubes (Figure 2A), which has been performed according to ref 5, spectra were taken immediately, one day and one week after the preparation of the CHQ nanotubes. The latter has been produced by evaporation of the solvent from a solution of nontubular CHQ in C₃D₆O and water. As can be seen from the spectrum in Figure 2A, the intensity of the peak at 0.5 ppm corresponding to methyl protons of initially deuterated acetone C₃D₆O grows during the experiment. The assignment of the peaks is taken from Hoffmann et al.⁵ While the peak of the protons of the OH groups cannot be clearly resolved in the solid-state NMR experiment, they are well-resolved in the corresponding solution ¹H NMR experiment (Figure 2B) on nontubular, but partially aggregated CHQ

* To whom correspondence should be addressed. E-mail: zakharov@theochem.uni-frankfurt.de, amasunov@mail.ucf.edu, andreas.dreuw@theochem.uni-frankfurt.de

[†] Institute of Physical and Theoretical Chemistry, Goethe University.

[‡] NMR Division, Max Planck Institute for Polymer Research.

[§] Nanoscience Technology Center, Department of Chemistry, and Department of Physics, University of Central Florida.

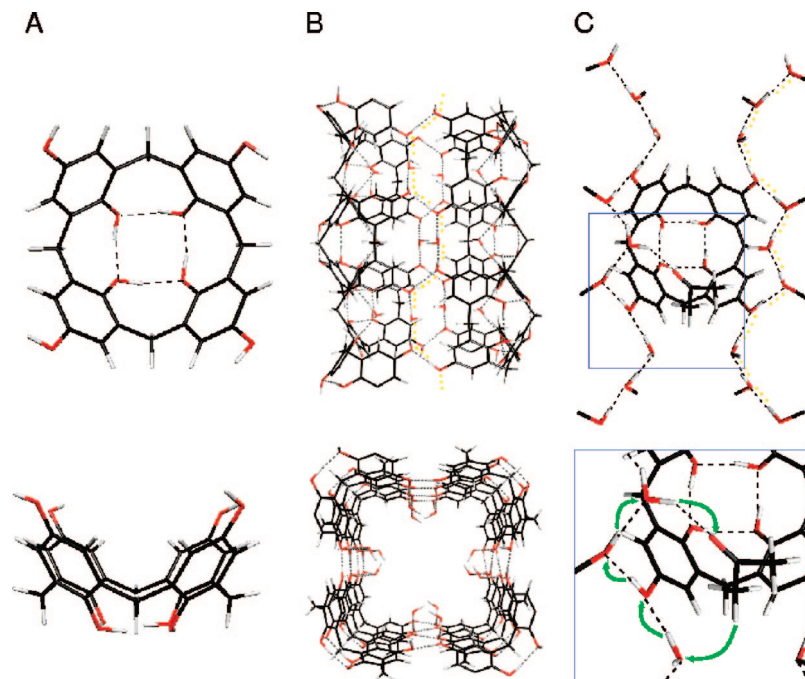


Figure 1. CHQ monomers (A), tubular CHQ (B), and fragment of tubular CHQ trapping acetone molecules (C), where the rest of the nanotube is removed for clarity. The 1D-H-bonded chain is highlighted by a yellow dotted line and a possible proton transport pathway is indicated by green arrows (C, bottom).

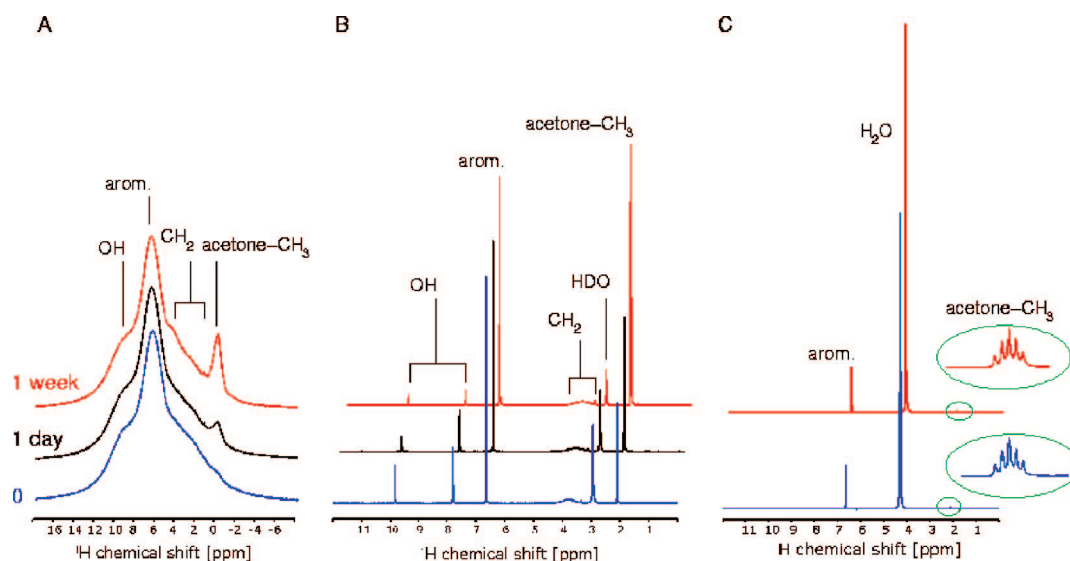
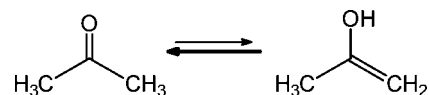


Figure 2. Solid state ^1H NMR spectrum of tubular CHQ trapping $\text{C}_3\text{D}_6\text{O}$ (A), solution ^1H NMR spectrum of CHQ dissolved in $\text{C}_3\text{D}_6\text{O}$ (B), and solution ^1H NMR spectrum of a mixture of QH_2 , $\text{C}_3\text{D}_6\text{O}$, and H_2O (C).

molecules in deuterated acetone. In the spectrum, a peak at about 3 ppm is visible corresponding to water impurities. The time evolution of the solution ^1H NMR spectrum reveals that the concentration of water protons decreases simultaneously with the increase of acetone methyl protons. According to these data, a proton–deuteron exchange between water and acetone takes place and, most likely, deuterated water subsequently exchanges deuterons with the OH-groups of the CHQ molecules, resulting in the observed decrease of their signals in the solution ^1H NMR spectrum. Since the proton exchange between acetone and water is observed in tubular aggregates of CHQ as well as in partially aggregated CHQ solution, both possess the property to catalyze the proton exchange.

On the contrary, it is a well-established fact that acetone alone does not exchange protons with water at normal conditions at

SCHEME 1: Keto–Enol Tautomerism of Acetone



pH 7.⁷ However, one might suspect that the weak acidity of CHQ may be responsible for the proton exchange (PE), since acids are known to catalyze keto–enol tautomerism (KET).⁸ Acetone KET is an interconversion between isomeric forms (keto and enol forms) involving a formal proton migration and a double bond (π -electron) shift (Scheme 1). Since KET involves several protonation/deprotonation steps in solution, it is reasonable to assume that it plays also a role in the proton exchange observed in the above-described NMR experiments between water and acetone.

To corroborate the weak acidity of CHQ is not the origin of the PE, an analogous ^1H NMR experiment has been performed on a solution of hydroquinone (QH_2) in a deuterated acetone and water mixture (1:1). QH_2 has been chosen because it possesses a very similar chemical structure to CHQ and should act as a weak organic acid as well. Although the $\text{p}K_{\text{a}}$ value of CHQ is not available, since CHQ aggregates in aqueous solution immediately, arguments will be given later that this assumption is clearly justified. Returning to the corresponding NMR experiment, no proton exchange could be observed (Figure 2C). The spectrum taken after one week does not show any changes in the intensities of the peaks corresponding to the methyl group of $\text{C}_3\text{D}_6\text{O}$ or of the water protons. Thus, the reason for the catalytic activity of CHQ in acetone–water proton exchange cannot be its weak acidity alone.

In order to clarify the nature and the mechanism of the catalytic function of CHQ in acetone–water proton exchange, we have performed a thorough quantum chemical study employing state-of-the-art quantum chemical methodology. Since hydroquinone and CHQ exhibit similar acidity, but show a different catalytic function for acetone–water proton exchange, we will focus here on concerted PE mechanisms. Before we turn to the investigation of the influence of CHQ on the acetone–water PE mechanism, we will first study the concerted mechanism in neutral water by using a well-defined acetone–water cluster. In particular, we address the question of how many water molecules are necessary to optimally catalyze PE. Then we will investigate the influence of CHQ on that concerted mechanism.

2. Theoretical Methods

The description of proton transfer reactions calls for a quantum treatment of the electronic structure at a highly correlated level, in addition to their nuclear dynamics. Such calculations are presently not feasible, and one must resort either to low quality electronic structure and nuclear dynamics or to static calculations at correlated ab initio levels. We have chosen to take the latter route. Since the full CHQ–water–acetone complex is by far too large even for a comprehensive static description by means of correlated quantum chemical methodology, we must resort to molecular models. We have chosen hydroquinone as a model because it represents a substructure of CHQ and has been used in previous studies.⁹ The acidity can be expected to be essentially identical, since the OH groups of CHQ and QH_2 exhibit identical polarity. Mulliken charge analyses reveal partial charges of -0.57 on oxygen and 0.31 on hydrogen for both systems at the DFT/B3LYP/6-31G** level of theory. Since the polarity of the OH groups essentially determines the acidity of the compounds, one can assume that they exhibit similar $\text{p}K_{\text{a}}$ values of approximately 10. Furthermore, calculation of the deprotonation energies of QH_2 and CHQ at B3LYP/6-31G** level revealed that they have also essentially identical deprotonation energies of 361 and 369 kcal mol $^{-1}$, respectively. This verifies that QH_2 and CHQ have similar chemical properties in proton transfer processes. However, this is in contrast to the NMR experiments, where CHQ and QH_2 behave differently with respect to the observed PE. As we will see later, the different behavior can be traced back to the presence and absence of solvent water molecules in the three NMR experiments, which are crucial for the rates of PE, and not to different structural and/or electronic properties of CHQ and QH_2 .

The model systems comprise the whole range of noncovalent interactions, i.e., dispersion interactions and hydrogen bonding

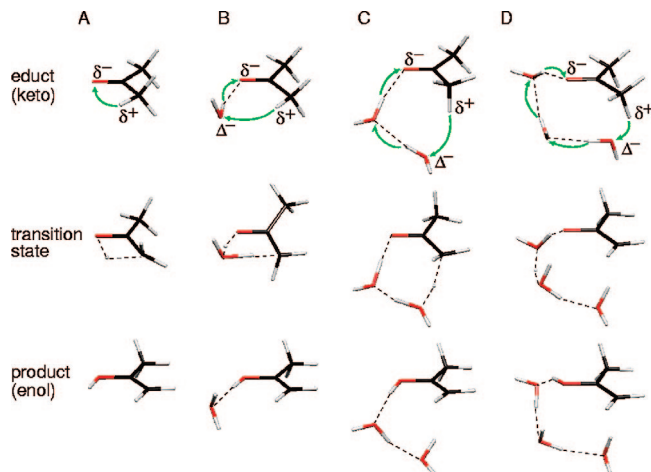


Figure 3. Molecular structures of the educts (top), transition states (middle), and products (bottom) along proton transfer pathways (green arrows) via keto–enol tautomerism in isolated acetone (A), acetone• H_2O (B), acetone• $2\text{H}_2\text{O}$ (C), and acetone• $3\text{H}_2\text{O}$ (D) clusters.

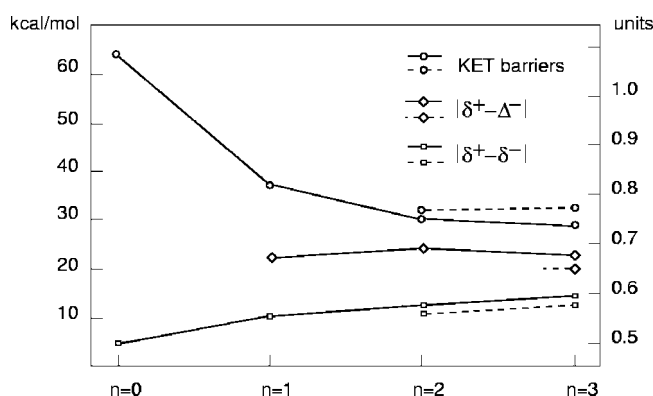
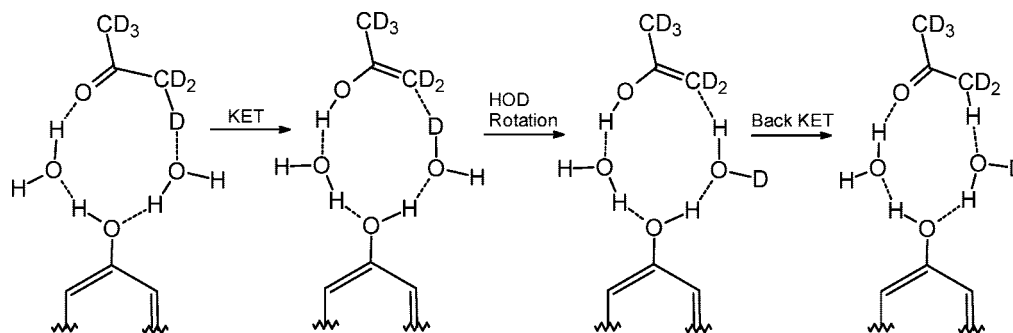


Figure 4. Zero-point energy corrected energy barriers of acetone–water proton transfer (circles) in $\text{C}_3\text{H}_6\text{O}\cdot n\text{H}_2\text{O}$, $n = 1-3$ (solid line) and $\text{QH}_2\text{--C}_3\text{H}_6\text{O}\cdot 2\text{H}_2\text{O}$ (dashed line) with respect to the number of participating OH-groups. The difference between the Mulliken charges at the acetone methyl hydrogen and carbonyl oxygen (squares) as well as between methyl hydrogen and the closest water oxygen (diamonds) in $\text{C}_3\text{H}_6\text{O}\cdot n\text{H}_2\text{O}$, $n = 1-3$ (solid line) and $\text{QH}_2\text{--C}_3\text{H}_6\text{O}\cdot 2\text{H}_2\text{O}$ (dashed line) are also given.

calling for high-level correlated ab initio methods. However, due to the size of the largest necessary model system, QH_2 with acetone and two water, the only applicable ab initio method is second order Møller–Plesset perturbation (MP2) theory.¹⁰ MP2 theory is capable to treat the long-range interactions with sufficient accuracy,¹¹ as well as the dispersion, polarization, and covalent effects associated with hydrogen bonding.¹² For the efficient location of transition state structures, as well as for the correction of proton transfer barriers by zero point vibrational energy (ZPVE), the computation of analytical second derivatives is required which restricts the largest possible basis set size to 6-31G** for the largest model systems (see, for example, Figure 4). Therefore, stationary point searches and harmonic vibrational frequencies of the majority of calculations were performed at the MP2 level with the moderate 6-31G** basis set, while energy barriers for proton transfer were improved by means of single point calculations with the larger cc-pVTZ basis set.¹³ Comparison with existing experimental and theoretical data demonstrates that our pragmatic approach is sufficiently quantitatively accurate for a meaningful investigation of the given systems.

Because the ZPVE correction is slightly overestimated within the harmonic approximation compared to that calculated with

SCHEME 2: Principal Mechanism of Proton Exchange via Concerted Keto-Enol Tautomerism (KET) of Acetone

corrected anharmonic potentials, we have scaled the harmonic ZPVE correction by a factor of 0.9.¹⁴

Another important issue in the calculation of supermolecular systems is basis set superposition error (BSSE) which leads to an overestimation of the stabilization energy and in mutilated potential energy surfaces of supermolecules. Since at correlated levels of theory, BSSE vanishes very slowly with increasing basis set size, its correction is necessary for a quantitative evaluation of stabilization energies of supermolecular complexes. One simple way of correcting BSSE is the Counterpoise (CP) procedure.¹⁵ The application of the CP correction within geometry optimizations at the MP2/6-31G** level gives structures and stabilization energies that are of similar quality to those obtained with much larger basis sets of triple- and quadruple- ζ quality and higher levels of theory like CCSD. Therefore, we employed the CP correction in geometry optimizations and stabilization energy calculations of several selected complexes.

MP2 natural orbital occupation number (NOON) analysis¹⁶ provides a useful criterion of the multireference nature of wave functions, which can become relevant during bond-breaking reactions and, hence, should be utilized in the proton transfer calculations. However, the NOON analysis of all transition state structures did not reveal any deviations from single-reference character. Hence, the closed-shell MP2 calculations with a single reference are clearly adequate for the study of all model systems.

In some cases, where the long-range interactions were not a major concern, we resorted to density functional theory (DFT)¹⁷ calculations with the common B3LYP functional¹⁸ and the 6-31G** basis. Primarily, the DFT approach was used to calculate the deprotonation energy and Mulliken charge distribution of CHQ monomers at different sites. We have also employed other approaches to compute partial charges for most investigated complexes, e.g., Löwdin charges, NBO charges, as well as partial charges from electrostatic potential fitting procedures as implemented in Gaussian 03. However, since they give essentially identical results, we can rely on straightforward Mulliken charge analyses in our discussion.

Most of the calculations were performed within the GAMESS-US¹⁹ software package, and computations of stabilization energies on CP-corrected potential energy surfaces and charges were done employing the Gaussian03 package of programs.²⁰

3. Concerted Proton Exchange in Calix[4]hydroquinone

A previous study of tubular CHQ structures employing solid-state NMR and quantum chemical calculations has given strong evidence that only one acetone molecule is trapped within one CHQ building block.^{5a} According to the derived structural model, the acetone molecule appears to be connected to the 1-D H-bond chain of the CHQ tubes via an additional H-bond from the carbonyl group of the acetone to the bridging water

molecule. One particularly favorable possibility for such a connection is given in Figure 1. Here, a water molecule is in the vicinity of the methyl group of acetone and several OH groups, which belongs either to water or CHQ and which establishes the 1-D H-bond chain, and can form a cyclic network. Within this network, all OH groups act as proton donors and acceptors simultaneously, and hence, they can efficiently assist proton transfer between the moieties.

Since the OH-groups of CHQ and water molecules are the key players in the observed PE of acetone and water, let us discuss in more detail the differences between the tubular and nontubular CHQ aggregates used in the previously described NMR experiments (A) and (B) shown in Figure 2. Within the solid state NMR experiment (A), most of the present water is bound as bridging water molecules within the 1D networks and only a negligible amount of “free” water is available. Therefore, it is justified to assume that in tubular CHQ, rather simple proton transfer networks exist comprising acetone connected by its carbonyl group to one of the –OH groups of bridging water or CHQ molecules. This has been suggested by an analysis of previous NMR experiments on CHQ nanotubes.^{5a} In the solution NMR experiment of Figure 2B, nontubular CHQ aggregates were formed and water molecules were present only as impurities. Here, one can also suppose that the limited number of water molecules in the sample mediates aggregation and is thus most likely bound to CHQ as bridging water. Therefore, one can, in tubular and nontubular aggregates of CHQ, assume that acetone molecules are part of very specific hydrogen bonding networks responsible for the observed PE between acetone and water. The basic mechanism of PE in tubular and nontubular aggregates of CHQ can thus be expected to be closely related.

As we have argued previously, the displayed NMR experiments point to the relevance of *concerted* proton exchange (PE) via KET involving several OH groups of bridging water and CHQ, in contrast to acid-catalyzed KET, which requires the dissociation of an OH-group prior to PE, which results in the generation of charged intermediates. Our general idea of the mechanism of PE via concerted KET is shown in Scheme 2. As a first step, it is assumed that a concerted keto–enol tautomerism mediated by two water molecules takes place, which transfers a deuteron from the methyl group of acetone to the H-bonded water. This particular water molecule is assumed to rotate and back-KET to take place. The rotation of the deuterated water molecule is essentially barrier-free at room temperature, since no chemical bond needs to be broken and the hydrogen bond to the methylene group is very weak. The final back-KET step is fast, since the keto-form is more stable than the enol form of acetone. Therefore, the initial KET step and the concomitant concerted transfer of the methyl deuteron

will determine the observed proton exchange rate between acetone and water.

3.1. Keto–Enol Tautomerism via Concerted Proton Transfer in Hydrated Acetone Clusters. As a first step in our investigation of the concerted PE mechanism catalyzed by CHQ, we investigated the KET mechanism of acetone catalyzed by water molecules alone. This is important if we want to understand the influence of CHQ on that mechanism. In this preliminary investigation, we are particularly interested in answering the question: how many catalytic water molecules, i.e., how many donor–acceptor OH-groups, are optimal to catalyze acetone KET? Furthermore, the influence of solvating water molecules not participating in the concerted KET mechanism is studied. This gives insight into the energetics and molecular details of the mechanism of concerted KET, and allows for identification of differences when CHQ comes into play.

To address the question of whether an optimal number of catalytic water molecules exists for concerted KET of acetone in water, we have composed hydrated $\text{C}_3\text{H}_6\text{O}\cdot n\text{H}_2\text{O}$ ($n = 0–3$) (Figure 3). They include cyclic proton transfer networks in complexes which each water acts as a proton donor and a proton acceptor simultaneously to make concerted KET possible. The geometries of these clusters have been optimized at the MP2/6-31G** level of theory in both the keto and enol forms as well as in the transition states.

The computed energy difference between the keto and enol forms of acetone itself is 11.3 kcal mol^{−1} at the MP2/cc-pVTZ//MP2/6-31G** level of theory and increases slightly to 11.6 kcal mol^{−1} when the zero point energy correction is employed. This agrees very favorably with a previous CPMD study at the BLYP level of theory, which gave 11.8 kcal mol^{−1}.^c Unfortunately, no experimental nor benchmark theoretical data is available to directly evaluate our computed values for the acetone–water cluster with one to three water molecules. Instead, we computed the averaged ZPVE-corrected energy difference between keto and enol forms of all considered hydrated clusters $\text{C}_3\text{H}_6\text{O}\cdot n\text{H}_2\text{O}$ clusters ($n = 1–3$) to be 10.7 kcal mol^{−1}. Compared to the experimental value of 10.3 ± 0.4 kcal mol^{−1} found in the aqueous solution of acetone,⁸ the agreement is very good. Since the relative energies of the keto and enol forms are nicely reproduced by our chosen theoretical approach, this gives us confidence that we can also describe the proton transfer mechanism with this methodology.

For the computation of the barrier heights of the suggested KET mechanism via concerted double-, triple-, and quadruple-proton transfer in the $\text{C}_3\text{H}_6\text{O}\cdot n\text{H}_2\text{O}$ clusters, transition state optimizations have been performed at the same level of theory, and the obtained geometries are displayed in Figure 3 (middle row). For all of these structures, computations of the harmonic frequencies revealed one imaginary value corresponding to the concerted proton transfer pathway. Furthermore, the single-reference character of the transition structures has been checked by computations of NOON values, and indeed they indicate no multireference character, allowing for further use of single-reference MP2 theory. The computed activation energies, i.e., energy barrier heights for concerted KET, are given as the differences between the total energies of the equilibrium ground-state structures of the keto and enol forms and the total energy of the connecting transition state. The obtained values for the $\text{C}_3\text{H}_6\text{O}\cdot n\text{H}_2\text{O}$ clusters ($n = 0–3$) are compiled in Table 1.

The computed numbers for the activation energy E_a for concerted KET reveal a strong decrease of the reaction barrier height with increasing number of catalytic water molecules.

TABLE 1: ZPVE Corrected Activation Energies E_a (kcal mol^{−1}) for Concerted Keto–Enol Tautomerism in Cyclic $\text{C}_3\text{H}_6\text{O}\cdot n\text{H}_2\text{O}$ Clusters ($n = 0–3$) and the Energy Difference ΔE of Keto and Enol Forms as a Function of the Number of Catalyzing Water Molecules N at the Theoretical Level of MP2/cc-pVTZ//MP2/6-31G^a**

| n | 0 | 1 | 2 | 3 |
|-------------------|-------------|-------------|-------------|-------------|
| E_a (keto→enol) | 64.0 (+3.0) | 37.5 (+2.7) | 30.4 (+3.4) | 29.1 (+1.7) |
| E_a (enol→keto) | 52.4 (+3.3) | 26.5 (+2.6) | 20.9 (+4.3) | 17.6 (+2.9) |
| ΔE | 11.6 (−0.3) | 11.0 (+0.1) | 9.6 (−0.9) | 11.5 (−1.2) |

^a The contributions of ZPVE scaled by 0.9 for anharmonicity are given in brackets and have been computed at MP2/6-31G** level.

While the energy barrier for KET via proton transfer in isolated acetone has a height of 64 kcal mol^{−1}, it drops readily by 26.5 kcal mol^{−1} to only 37.5 kcal mol^{−1} with only one catalytic water molecule, and decreases further to only 30.4 and 29.1 kcal mol^{−1} with two and three catalytic water molecules at the theoretical level of MP2/cc-pVTZ//MP2/6-31G** including ZPVE. This is in agreement with a previous MP2 study,^{21b} which has demonstrated that one water molecule leads to a reduction of 26.1 kcal mol^{−1} of the activation energy for KET in acetone from 69.2 kcal mol^{−1} for isolated acetone itself to 43.1 kcal mol^{−1}.

In Figure 4A, the functional dependence of the activation energy, i.e., barrier height for concerted KET in acetone–water complexes on the number of catalytic water molecules is displayed. The barrier height is practically converged with three catalytic water molecules and one can expect only a minor further decrease when a fourth water molecule is embedded in the catalytic hydrogen network. On the contrary, one can expect the activation barrier to increase again with larger amounts of water molecules, i.e., in solution, since earlier computations employing self-consistent reaction field (SCRf) methodology to include solvent effects have shown that the solvent effects increase the activation energy by about 2 kcal mol^{−1} in the acetone–(H₂O) complex. In a recent Car–Parrinello molecular dynamics simulation of acetone keto–enol tautomerism in water solution,^{21c} the activation energy for KET has been computed to be 57.7 kcal mol^{−1} for isolated acetone in the gas phase and 38.5 kcal mol^{−1} for KET catalyzed by four water molecules in the presence of altogether 24 explicit solvent water molecules. It is worth noting that the employed DFT-based technique tends to underestimate reaction barriers, thus the barriers are most likely higher in reality, as is the case in our MP2 calculations. However, this indicates that the activation barrier for KET of acetone in aqueous solution is higher than that in isolated $\text{C}_3\text{H}_6\text{O}\cdot n\text{H}_2\text{O}$ complexes with well-defined and specific H-bond networks. In summary, these findings already indicate that solvent water molecules, i.e., water molecules that are not involved in the PT as proton-donor/proton-acceptor, supposedly decrease the efficiency of keto–enol tautomerism (KET). This is also in agreement with recent studies on tautomerism of various organic molecules, where solvent water was treated explicitly.²²

Our model computations offer the possibility to study the influence of solvent water molecules on the KET mechanism in great detail. Thus, we also studied the explicit influence of an additional solvent water molecule on the activation energy for KET in the acetone•H₂O complex, where KET is catalyzed by one water molecule and proceeds via concerted double proton transfer. For this purpose, we have constructed two additional acetone•2H₂O complexes, in which the second water molecule is not part of the catalytic H-bond network, but instead bound

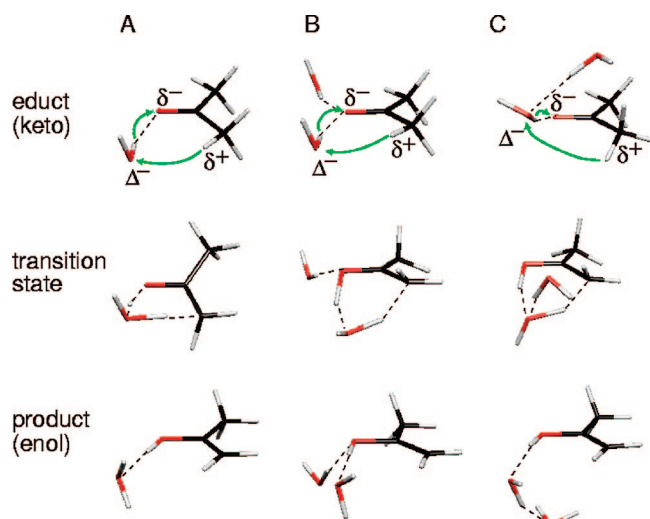


Figure 5. Optimized stationary structures of the educts (top), transition states (middle), and products (bottom) along the proton transfer pathways (green arrows) in acetone•H₂O (A), acetone•H₂O with one additional solvent water bound to acetone carbonyl (B), and acetone•H₂O with one additional solvent water bound to water oxygen.

additionally to the keto-group of acetone (isomer **A**) or to the oxygen of the single catalytic water (isomer **B**) (Figure 5). Again, the keto and enol forms of the two isomers of C₃H₆O•2H₂O as well as the transition states for concerted double proton transfer have been optimized. Harmonic frequency calculations reveal that the keto and enol forms represent local minima with only real frequencies, while the transition states exhibit one imaginary frequency. Computations of the activation energies for concerted KET via double proton transfer in isomers **A** and **B** reveal that the barrier heights for concerted KET are 37.7 and 40.7 kcal mol⁻¹, respectively, at the MP2/cc-pVTZ//MP2/6-31G** level including ZPVE correction. Comparison with the value for the C₃H₆O•H₂O complex without additional solvent water (Figure 5, left column) of 37.5 kcal mol⁻¹ reveals that the barrier is increased by 3.2 kcal mol⁻¹ only when the solvent water is bound to the catalytic water. Obviously, hydrogen bonding to the catalytic water reduces its catalytic activity, while hydrogen bonding to the acetone carbonyl group has only negligible influence. This indicates that, in principle, only such solvent water molecules which directly bind the catalytic H-bond networks increase the KET energy barrier and thereby decrease the catalytic efficiency. While the first solvent water molecule directly bound to the catalytic water network appears to have an influence of approximately 3 kcal mol⁻¹, further water molecules will still lead to an increase of the barrier, but to a smaller extent. However, this remains to be shown in detail and is currently only hypothetical (Table 2).

The natural question to ask now is why the two solvent molecules in isomer **A** and **B** behave so differently. To answer that question, one first must go one step back and consider the role of the catalytic water molecules, i.e., what influence on these water molecules leads to catalysis. The answer to the latter question is most importantly polarization of acetone. The more strongly polarized the acetone molecule becomes, i.e., the more partial positive charge becomes located on the hydrogens of the methyl groups and the more negative charge becomes located on the carbonyl oxygen, the more likely acetone becomes to accept a proton at the carbonyl oxygen and to donate a proton from the methyl group. One simple way to quantify the polarization of acetone is by the difference of the partial charges

TABLE 2: ZPVE Corrected Activation Energies E_a (kcal mol⁻¹) for Concerted Keto–Enol Tautomerism in QH₂–C₃H₆O•H₂O ($n = 2$) and QH₂–C₃H₆O•2H₂O ($n = 3$) and the Energy Difference ΔE of Keto and Enol Forms As Function of the Number of Catalyzing Hydroxyl Groups N at the Theoretical Level of MP2/cc-pVTZ//MP2/6-31G.^a**

| n | 2 | 3 |
|-------------------|-------------|-------------|
| E_a (keto→enol) | 31.9 (−2.4) | 32.2 (−3.4) |
| E_a (enol→keto) | 7.4 (−2.9) | 18.5 (−3.5) |
| ΔE | 24.5 (+0.5) | 13.7 (+0.1) |

^a The contributions of ZPVE scaled by 0.9 for anharmonicity are given in brackets and have been computed at MP2/6-31G** level.

on the carbonyl oxygen and methyl hydrogens. In Figure 4B, the dependence of the difference between the partial charges on the proton-accepting carbonyl oxygen and proton-donating methyl group of acetone on the number of catalytic water molecules is given. It is apparent that the polarization of acetone is converged in the same way that the height of the reaction barrier for concerted KET is converged when approximately three to four catalytic water molecules are involved. Thus, a clear connection between acetone polarization and barrier height for concerted KET can be derived.

A closer look at the structures of the acetone• n H₂O complexes with up to three catalytic water molecules (Figure 3) explains why the activation energy converges to an optimal value with possibly three to four water molecules. An increase in the size of the cyclic H-bond network at some point no longer leads to an increased polarization of acetone, since a cooperative, i.e., an additive effect of the water dipoles, is diminished due to several structural factors. The catalytic water molecules have to arrange in structures, which are far from linear in alignment, allowing for optimal polarization, and the distance between the catalytic water molecules and acetone increases with an increasing number of catalytic water molecules.

Extrapolating our results to KET of acetone in neutral aqueous solution, one can make a rough estimate on the energetics. Suppose the most efficient KET process with a barrier of ~30 kcal mol⁻¹ assisted by three or, perhaps, four water molecules in an isolated acetone–water complex, as we have studied them. Solvation of this cluster in water will lead to hydrogen bonding of the catalytic water molecules, decreasing their ability to polarize acetone. If we assume each catalytic water molecule to be H-bonded by a solvent water molecule and if we further assume that each solvated catalytic water molecule adds about 3 kcal mol⁻¹ to the minimal barrier of 30 kcal mol⁻¹, then one would arrive at an activation energy for KET of acetone in water of about 40 kcal mol⁻¹. This is consistent with the value of 38.5 kcal mol⁻¹ obtained from the CPMD simulation described previously,^{21c} where on average 4 water molecules catalyzed the KET in the presence of 24 solvent water molecules.

Returning to CHQ and the initially described NMR experiments, the ones in which acetone–water PE has been observed have been performed under conditions with no or only very little free water that could act as solvent water to increase the activation energy for KET. Thus, based on our results for acetone–water clusters, one can expect concerted acetone KET to be more efficient by about 10 kcal mol⁻¹ in CHQ with proton transfer networks similar to our model system than that found in aqueous solution.

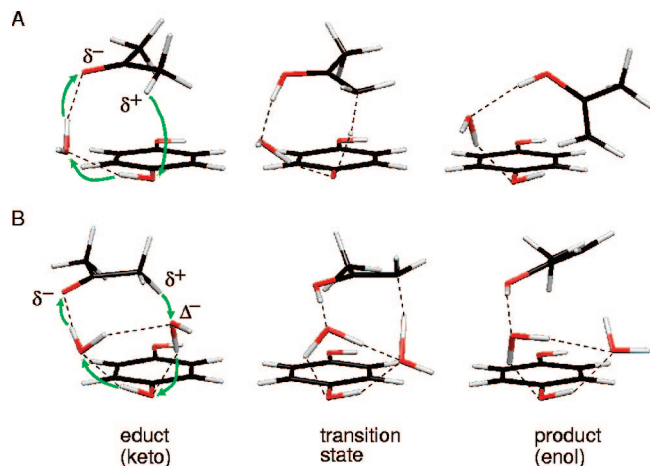


Figure 6. Optimized educt (left), transition state (center), and product (right) structures of the QH_2 –acetone• $2\text{H}_2\text{O}$ model complex (A) and QH_2 –acetone• $2\text{H}_2\text{O}$ model complex (B) along the concerted acetone keto–enol tautomerism (green arrows).

3.2. Keto–Enol Tautomerism in Hydrated Hydroquinone–Acetone Clusters. Now that we have understood the mechanism of acetone KET catalyzed by H-bond networks in acetone–water complexes in great detail, the next logical step is to investigate the influence of CHQ on the concerted KET of acetone. The basic question to answer is how the activation energy barrier changes when one of the OH groups of the H-bond networks stems from CHQ and not from water. Since CHQ is too large to afford calculations at the MP2 level even with only medium-sized basis sets, in all model calculations hydroquinone (QH_2) was used as the model system (see Section 2).

As a first step, we composed two model complexes consisting of QH_2 , acetone, and one or two catalyzing water molecules, which, as closely as possible, resemble the structure predicted in previous NMR experiments.⁵ The geometries of these model complexes have been optimized at the MP2/6-31G** level of theory, and the stable stationary points corresponding to keto and enol forms and the transition state in the QH_2 – $\text{C}_3\text{H}_6\text{O}$ • $2\text{H}_2\text{O}$ cluster with two catalytic water molecules are shown in Figure 6.

The smaller cluster with only one catalytic water molecule exhibits two OH- groups that are involved in the concerted KET mechanism, one from QH_2 and the other from the catalytic water. The results for that cluster have thus to be compared with those for acetone• $2\text{H}_2\text{O}$, since in the latter two catalytic OH-bonds (both from water) are also involved. Computation of the energies of the keto and enol forms and the transition state along the concerted KET pathway of the QH_2 – $\text{C}_3\text{H}_6\text{O}$ – H_2O cluster, gives values for the activation energy for concerted KET of $31.9 \text{ kcal mol}^{-1}$ at MP2/cc-pVTZ//MP2/6-31G** level of theory, which is $1.5 \text{ kcal mol}^{-1}$ higher than in the acetone• H_2O cluster. The relative energy between keto and enol forms of this cluster is $7.4 \text{ kcal mol}^{-1}$. In the larger QH_2 – $\text{C}_3\text{H}_6\text{O}$ • $2\text{H}_2\text{O}$ cluster, the activation energy for concerted KET via quadruple proton transfer according to Figure 6 is found to be even higher with $32.7 \text{ kcal mol}^{-1}$ at the MP2/cc-pVTZ//MP2/6-31G** level of theory. Compared to the corresponding value for the acetone• $2\text{H}_2\text{O}$ cluster exhibiting concerted KET via quadruple proton transfer of $29.1 \text{ kcal mol}^{-1}$, substitution of one water by an OH-group of QH_2 increases the activation energy by $3.6 \text{ kcal mol}^{-1}$. Obviously, concerted KET of acetone is less efficient in the QH_2 clusters than in the analogous water clusters.

Having understood the catalytic function of the water molecules in the acetone–water clusters as polarizing agents, the slightly less efficient catalytic function QH_2 compared to

water is readily explained in terms of the different polarity of the OH groups of QH_2 and water. Indeed, the OH-group of QH_2 is slightly less polar than the –OH group of water, which is indicated by Mulliken charge differences between oxygen and hydrogen of 0.73 and 0.60 in H_2O and QH_2 , respectively, at the MP2/cc-pVTZ//MP2/6-31G** level. Therefore, it is also unnecessary to consider model clusters in which both OH-groups of QH_2 are involved. In summary, in the case of QH_2 – $\text{C}_3\text{H}_6\text{O}$ • H_2O , the two OH-groups of the catalytic water and QH_2 are slightly less efficient in polarizing the acetone than two water OH-groups, as in case of $\text{C}_3\text{H}_6\text{O}$ • $2\text{H}_2\text{O}$. This is also nicely illustrated in Figure 4 by the relation of the partial charges on the carbonyl oxygen and methyl hydrogen atoms of acetone and the corresponding values of the activation energies for concerted KET in QH_2 – $\text{C}_3\text{H}_6\text{O}$ • H_2O and $\text{C}_3\text{H}_6\text{O}$ • $2\text{H}_2\text{O}$ clusters.

It is at first glance surprising that a second catalytic water molecule readily increases the activation energy in the QH_2 – $\text{C}_3\text{H}_6\text{O}$ – H_2O clusters for concerted KET of acetone. However, as can be seen in Figure 6, the catalytic water molecules in the QH_2 – $\text{C}_3\text{H}_6\text{O}$ • $2\text{H}_2\text{O}$ model complexes are H-bonded among each other in the vicinity of the acetone methyl group. This again leads to a depolarization of the acetone molecule, and having this in mind, one can state that the second catalytic water also acts as a solvent water, thereby not leading to a significant change in the efficiency of the KET process.

Let us finally compare the stabilization energies of the QH_2 – $\text{C}_3\text{H}_6\text{O}$ • H_2O (Figure 6, A) and $\text{C}_3\text{H}_6\text{O}$ • $2\text{H}_2\text{O}$ (Figure 3, C) clusters, since this gives an idea of the strength and compactness of the H-bond networks. We have seen that both clusters have similar activation energies for KET via concerted triple proton transfer of 31.9 and $30.4 \text{ kcal mol}^{-1}$, respectively. To obtain meaningful stabilization energies, the CP correction has been employed and both structures have been reoptimized on CP-corrected potential energy surfaces. Also, zero point energy correction has been calculated with the CP correction included. Using this approach, at the level of CP-corrected MP2/6-31G** we obtain values for the stabilization energies for QH_2 – $\text{C}_3\text{H}_6\text{O}$ • H_2O and $\text{C}_3\text{H}_6\text{O}$ • $2\text{H}_2\text{O}$ of -12.6 and $-8.4 \text{ kcal mol}^{-1}$, respectively, i.e., QH_2 – $\text{C}_3\text{H}_6\text{O}$ • H_2O is $4.2 \text{ kcal mol}^{-1}$ more strongly bound than $\text{C}_3\text{H}_6\text{O}$ • $2\text{H}_2\text{O}$. At the level of single point CP-corrected MP2 energy calculations with a cc-pVTZ basis set, the difference is even slightly larger and amounts to $5.7 \text{ kcal mol}^{-1}$. Although the efficiency of catalysis of the KET via the OH group of QH_2 and water is slightly weaker than the catalysis by two water OH groups alone, one can conclude that the stability of proton transfer networks is considerably larger in the QH_2 complex—by about one H-bond strength of water dimer (4.0 to $5.7 \text{ kcal mol}^{-1}$), which is most likely due to dispersion interactions between the aromatic ring of QH_2 , acetone, and water. Going to CHQ, one would expect that these dispersion interactions become even larger due to the increased number of aromatic rings, and the H-bond network in the CHQ cages are even stronger and more compactly bound. As a result, this will lead to the specific structures of 1D H-bond chains, as described previously, and to the efficient trapping of one acetone per CHQ subunit in tubular and nontubular CHQ aggregates, thereby also explaining the observed efficient binding of other small organic molecules by CHQ.⁵

Summary and Conclusions

In this work, we have investigated the mechanism of the catalytic proton exchange between acetone and water in tubular and nontubular CHQ aggregates as it has been observed in NMR experiments by means of quantum chemical ab initio calcula-

tions. Our working hypothesis derived from the NMR data was that the proton exchange proceeds via concerted keto–enol tautomerism (KET) of trapped acetone molecules and that acid catalysis does not play a role.

As a first step, we have studied concerted KET of acetone in specific clusters with one to three water molecules. The KET process has been shown to proceed via concerted double, triple, and quadruple proton transfer. In particular, we could show that three or even four water molecules are probably optimal for the catalysis of KET, and that the activation energy of this process is about 30 kcal mol⁻¹, which is about 10 kcal mol⁻¹ lower than that in aqueous solution. To explain this discrepancy, we have then also studied the influence of solvent water molecules on the KET mechanism. We were able to show that H-bonding of a catalytic water molecule by a solvent water molecule leads to an increase of the activation energy for concerted KET of about 3 kcal mol⁻¹. The reason for this increase in the activation energy could be traced back to a diminished polarization of the acetone by the catalytic water molecules in the presence of the solvent waters. Thus, concerted KET is more efficient in solvent-free environments with only a few catalytic water molecules.

Having understood the mechanism of concerted KET of acetone in water in detail, we turned to the investigation of the influence of CHQ. For this objective, we have used model complexes comprising hydroquinone (QH₂), which served as a molecular model for CHQ, acetone, and one or two catalytic water molecules. Our calculations revealed that concerted KET via double or quadruple proton transfer in these model complexes is slightly less efficient than that in the corresponding acetone–water complexes. Basically, this is because of the lower polarity of the OH-group of QH₂ compared to that of water. Finally, we have computed stabilization energies for the acetone–water and QH₂–acetone–water complexes, and we were able to demonstrate that the hydrogen networks in the latter complex are significantly stronger bound than those in the former.

Acetone–water proton exchange in superheated water can be quantitatively explained by the mechanism found in the present study. In an NMR experiment,⁷ proton exchange between acetone and superheated deuterated water was achieved at 200 °C during a total exposure time of 60 min. This agrees nicely with our calculated rate constant at 473 K of about 10⁻¹ M⁻¹ s⁻¹, which would allow for the observation of proton exchange under these conditions. However, the rate constant for concerted KET obtained using the activation energy of the most efficient case C₃H₆O•3H₂O of 29.1 kcal mol⁻¹ is 10⁻¹³ M⁻¹ s⁻¹ at room temperature. This is clearly too low to explain the observation of proton exchange at the conditions of the NMR experiment. Thus, we can conclude that at room temperature, KET via concerted proton transfer, assisted by a few OH-groups, is no longer the prevailing mechanism of the proton exchange, catalyzed by CHQ.

Although we were not able to identify the KET mechanism of the catalytic activity of CHQ, we have found that desolvation of the proton-transfer networks assisting KET appears to be a very important, if not crucial, feature of CHQ.

Future investigations of the mechanism of proton-exchange in CHQ will have to consider the dissociation of the CHQ OH-groups and the concomitant formation of charged species. These studies are currently underway.

Acknowledgment. Authors acknowledge Dr. Anke Hoffmann for providing the experimental materials. A.D. is funded by the

Deutsche Forschungsgemeinschaft as an Emmy Noether fellow. A.E.M.'s work is supported, in part, by the National Science Foundation's program Collaborative Research in Chemistry, Award No. 0832622.

References and Notes

- (1) (a) Harada, A.; Li, J.; Kamachi, M. *Nature* **1993**, *364*, 516. (b) Ghadiri, M. R.; Granja, J. R.; Milligan, R. A.; McRee, D. E.; Khazanovich, N. *Nature* **1993**, *366*, 324. (c) Feldman, Y.; Wasserman, E.; Srolovitz, D.; Tenne, R. *Science* **1995**, *267*, 222. (d) Barbour, L.; Orr, G. W.; Atwood, J. L. *Nature* **1998**, *393*, 671. (e) Fenniri, H.; Mathivanan, P.; Vidale, K. L.; Sherman, D. M.; Hallenga, K.; Wood, K. V.; Stowelet, J. G. *J. Am. Chem. Soc.* **2001**, *123*, 3854.
- (2) (a) Hong, B. H.; Lee, J. Y.; Kim, J. C.; Bae, S. C.; Kim, K. S. *J. Am. Chem. Soc.* **2001**, *123*, 10748. (b) Kim, K. S.; Suh, S. B.; Kim, J. C.; Hong, B. H.; Lee, E. C.; Yun, S.; Tarakeshwar, P.; Lee, J. Y.; Kim-Ihm, H.; Kim, H. G.; Lee, J. W.; Kim, J. K.; Lee, H. M.; Kim, D.; Cui, C.; Youn, S. J.; Chung, H. Y.; Choi, H. S.; Lee, C.-W.; Cho, C. J.; Jeong, S.; Cho, J.-H. *J. Am. Chem. Soc.* **2002**, *124*, 14268.
- (3) (a) Hille, B. *Ionic Channels of Excitable Membranes*; Sinauer: Sunderland, MA; 1984. (b) Ghadiri, M. R.; Granja, J. R.; Buehler, L. *Nature* **1994**, *369*, 301.
- (4) Kim, K. S. *Bull. Korean Chem. Soc.* **2003**, *24*, 6–757.
- (5) (a) Hoffman, A.; Sebastiani, D.; Sugiono, E.; Yun, S.; Kim, K. S.; Spiess, H.-W. *Chem. Phys. Lett.* **2004**, *388*, 164. (b) Brunklaus, G.; Koch, A.; Sebastiani, D.; Spiess, H.-W. *Phys. Chem. Chem. Phys.* **2007**, *9*, 4545–4551.
- (6) Hoffman, A., Private Communication.
- (7) Kuhlmann, B.; Arnett, E. M.; Siskin, M. *J. Org. Chem.* **1994**, *59*, 3098.
- (8) Chiang, Y.; Kresge, A. J.; Shepp, N. P. *J. Am. Chem. Soc.* **1989**, *111*, 3977.
- (9) Manojkumar, T. K.; Kim, D.; Kim, K. S. *J. Chem. Phys.* **2005**, *122*, 14305.
- (10) (a) Møller, C.; Plesset, M. S. *Phys. Rev.* **1934**, *46*, 618. (b) Pople, J. A.; Binkley, J. C.; Seeger, A. *Int. J. Quantum Chem.* **1976**, *S10*, 1.
- (11) Van Mourik, T.; Wilson, A. K. *Mol. Phys.* **1999**, *96*, 529.
- (12) Xantheas, S. S.; Arpa, E. *J. Chem. Phys.* **2004**, *120*, 823.
- (13) Dunning, T. H. *J. Chem. Phys.* **1989**, *90*, 1007.
- (14) Dykstra, C. E.; Shuler, K.; Young, R. A.; Bacic, Z. *J. Mol. Struct. THEOCHEM* **2002**, *591*, 11.
- (15) Boys, S. F.; Bernnardi, F. *Mol. Phys.* **1970**, *19*, 553.
- (16) (a) Pulay, P.; Hamilton, T. P. *Chem. Phys.* **1988**, *88*, 4926. (b) Gordon, M. S.; Schmidt, M. W.; Chaban, G. M.; Glaesmann, K. R.; Stevens, W. J.; Gonzales, C. J. *Chem. Phys.* **1999**, *110*, 4199.
- (17) (a) Parr, R. G.; Yang, W. *Density-Functional Theory of Atoms and Molecules*; Oxford University Press: New York; 1989. (b) Kohn, W.; Becke, A. D.; Parr, R. G. *J. Phys. Chem.* **1996**, *100*, 12974.
- (18) (a) Becke, A. D. *Phys. Rev. A* **1988**, *38*, 3098. (b) Lee, C.; Yang, W.; Parr, R. G. *Phys. Rev. B* **1988**, *37*, 785.
- (19) Schmidt, M. W.; Baldridge, K. K.; Gordon, M. S.; Jensen, J. H.; Koseki, S.; Matsunaga, N.; Nguyen, K. A.; Su, S.; Windus, T. L.; Dupius, M.; Montgomery, J. A. *J. Comput. Chem.* **1993**, *14*, 1347.
- (20) *Gaussian 03, Revision C.02*; Frisch, M. J.; Trucks, G. W.; Schlegel, H. B.; Scuseria, G. E.; Robb, M. A.; Cheeseman, J. R.; Montgomery, Jr. A.; Vreven, T.; Kudin, K. N.; Burant, J. C.; Millam, J. M.; Iyengar, S. S.; Tomasi, J.; Barone, V.; Mennucci, B.; Cossi, M.; Scalmani, G.; Rega, N.; Petersson, G. A.; Nakatsuji, H.; Hada, M.; Ehara, M.; Toyota, K.; Fukuda, R.; Hasegawa, J.; Ishida, M.; Nakajima, T.; Honda, Y.; Kitao, Y.; Nakai, H.; Klene, M.; Li, X.; Knox, J. E.; Hratchian, H. P.; Cross, J. B.; Bakken, V.; Adamo, C.; Jaramillo, J.; Gomperts, R.; Stratmann, R. E.; Yazyev, O.; Austin, A. J.; Cammi, R.; Pomelli, C.; Ochterski, J. W.; Ayala, P. Y.; Morokuma, K.; Voth, G. A.; Salvador, P.; Dannenberg, J. J.; Zakrzewski, V. G.; Dapprich, S.; Daniels, A. D.; Strain, M. C.; Farkas, O.; Malick, D. K.; Rabuck, A. D.; Raghavachari, K.; Foresman, J. B.; Ortiz, J. V.; Cui, Q.; Baboul, A. G.; Clifford, S.; Cioslowski, J.; Stefanov, B. B.; Liu, G.; Liashenko, A.; Piskorz, P.; Komaromi, I.; Martin, R. L.; Fox, D. J.; Keith, T.; Al-Laham, M. A.; Peng, C. Y.; Nanayakkara, A.; Challacombe, M.; Gill, P. M. W.; Johnson, B.; Chen, W.; Wong, M. W.; Gonzalez, C.; and Pople, J. A.; Gaussian, Inc., Wallingford CT, 2004.
- (21) (a) Noack, W.-E. *Theor. Chim. Acta.* **1979**, *53*, 101. (b) Lee, D.; Kim, C. K.; Lee, B.; Lee, I. *J. Comput. Chem.* **1997**, *18*, 56. (c) Cucinotta, C. S.; Ruini, A.; Catellani, A.; Stirling, A. *Chem. Phys. Chem.* **2006**, *7*, 1229.
- (22) (a) Hu, X.; Li, H.; Liang, W.; Han, S. *J. Phys. Chem. B* **2004**, *108*, 12999–13007. (b) Liang, W.; Li, H.; Hu, X.; Han, S. *J. Phys. Chem. A* **2004**,